ACR No. L5A11

NATIONAL ADVISORY COMMITTEE FOR AERONAUTICS

WARTIME REPORT

ORIGINALLY ISSUED

January 1945 as
Advance Confidential Report L5A11

THE EFFECT OF TRAILING-EDGE EXTENSION FLAPS ON PROPELLER CHARACTERISTICS

By John L. Crigler

Langley Memorial Aeronautical Laboratory
Langley Field, Va.

NACA

WASHINGTON

NACA ACR No. L5A11 [redacted]

NATIONAL ADVISORY COMMITTEE FOR AERONAUTICS

ADVANCE CONFIDENTIAL REPORT

THE EFFECT OF TRAILING-EDGE EXTENSION FLAPS ON PROPELLER CHARACTERISTICS

By John L. Crigler

SUMMARY

An analysis was made to determine the effect on propeller performance of extension flaps added to the trailing edge of a propeller blade. A method of calculating the changes in the ideal angle of attack, the angle of zero lift, and the design lift coefficient of a propeller blade section having a trailing-edge extension flap was utilized to calculate the performance of a six-blade dual-rotating propeller with extension flaps varying up to 40 percent chord. The method was used to determine the angle that the flap extension must make with the chord in order to obtain a particular load distribution. Although the analysis in this report was made for a wind-tunnel propeller designed to operate at low advance-diameter ratio, the method is directly applicable to any propeller section under any operating condition.

INTRODUCTION

Inasmuch as the production of a propeller of a given design is an expensive manufacturing procedure, it is expedient to make each existing design useful for as many applications as possible. For this reason, several choices of diameter have been available with a given blade design. This flexibility of design has recently been increased by providing a procedure for adding an extension along the blade. The selection of the width of extension permits a choice of propeller solidity for a given blade design and diameter. The addition of the trailing-edge extension changes the section airfoil characteristics by an amount dependent

on the length and angle of extension. Some choice in the airfoil characteristics is therefore permitted when the extension flap is added to the trailing edge. Reference 1 presents a method of analyzing the change in airfoil section characteristics accompanying changes in extension length and angle, and the present report applies the method of reference 1 to the calculation of propeller characteristics.

The calculations given herein were made for a six-blade dual-rotating propeller for values of advance-diameter ratio (V/nD) that are encountered in the operation of a propeller used to drive a wind tunnel. The same methods are applicable, however, to propellers for any operating condition. Preliminary calculations were first made on the propeller with the original blades in order to study the distribution of loading along the blade for a power coefficient $C_P = 0.31$ at an advance-diameter ratio $V/nD = 0.33$. For this value of V/nD, the inboard sections of the propeller were found to stall before the outboard sections and, furthermore, the whole propeller was found to stall before a power coefficient of 0.31 was absorbed. In order to make the design suitable for these operating conditions, it was necessary to increase the solidity of the original propeller. Trailing-edge extension flaps were used for this purpose and were attached in such a manner as to change the angle of zero lift along the blade to increase the load on the outer sections. Inasmuch as the effect of such extension flaps is applicable to both tunnel and aircraft propellers, the method given herein for use in tunnel-propeller design may also be used in determining the effect of trailing-edge extension flaps on propeller sections for aircraft applications.

The method used to calculate the changes in the ideal angle of attack, the design lift coefficient, and the angle of zero lift resulting from a flat sheet attached to the trailing edge of an airfoil section is outlined in reference 1. This method was used to calculate the lift as a function of angle of attack for the sections of a six-blade dual-rotating propeller having Curtiss blades 836- and 837-102-13 with trailing-edge extension flaps. The calculated thrust- and torque-distribution curves for the propeller with a 40-percent-chord trailing-edge flap are presented for two operating conditions.

[redacted]

SYMBOLS

b	chord of propeller blade element
C_L	section lift coefficient $\left(\frac{L}{\frac{1}{2}\rho V^2 b}\right)$
C_{L_D}	section design lift coefficient; lift coefficient at ideal angle of attack
C_P	power coefficient $(P/\rho n^3 D^5)$
C_Q	torque coefficient $(Q/\rho n^2 D^5)$
C_T	thrust coefficient $(T/\rho n^2 D^4)$
D	propeller diameter
$\frac{dC_Q}{dx}$	element torque coefficient $\left(\frac{dQ/dx}{\rho n^2 D^5}\right)$
$\frac{dC_T}{dx}$	element thrust coefficient $\left(\frac{dT/dx}{\rho n^2 D^4}\right)$
h	thickness of propeller blade element
L	lift of blade section
M	Mach number
n	propeller rotational speed
p	geometric pitch of propeller
P	input power to propeller
Q	torque of propeller
r	radius to any blade element
R	tip radius
T	thrust of propeller

[redacted]

V	airspeed
x	radial location of blade element (r/R)
α	angle of attack
α_{l_o}	angle of zero lift
α_I	ideal angle of attack
β	propeller blade angle at 0.75 radius
θ	propeller blade angle at radius r
ρ	mass density of air

Subscripts:

F	front propeller
R	rear propeller
0.7	at 0.7 radius

ANALYSIS

The propeller analyzed is a six-blade dual-rotating propeller with Curtiss blades 836-102-13 (front, right hand) and 837-102-13 (rear, left hand). Blade-form curves for the propeller are given in figure 1. The propeller conditions analyzed vary from a value of $C_P = 0.31$ at $V/nD = 0.33$ to a value of $C_P = 0.095$ at $V/nD = 0.26$. Preliminary calculations showed that the propeller with the original blades would stall at an advance-diameter ratio of 0.33 before absorbing a power coefficient of 0.31. In order to use the available propeller for this condition, it was necessary to increase the propeller solidity by the use of extension flaps attached to the trailing edge. Extension flaps cause a change in the angle of zero lift, which results in an effective change in the propeller pitch distribution. It was necessary, therefore, to calculate the lift of the sections as a function of angle of attack for use on the propeller. The method of

[redacted]

reference 1 was used to calculate the change in lift characteristics caused by extension flaps, and the results show the angle that will be required between the extension flap and the chord line of the original airfoil to produce zero change in pitch distribution for several sections along the blade.

Certain assumptions regarding the airfoil characteristics of the propeller were necessary in order to make the calculations. Experimental data are usually used in analyzing propeller performance. Inasmuch as the Curtiss blades 836- and 837-1C2-13 are of NACA 16-series airfoil section, the section lift characteristics (fig. 2) for the original propeller were obtained by extrapolating the experimental data of reference 2. The design lift coefficients and the operating Mach numbers for several sections along the blade for the limiting condition of operation are shown in figure 2. The calculations for the sections with extension flaps were made on the assumption that the addition of flaps did not change the slope of the lift curve for a given section. Inasmuch as no experimental data were available for the airfoil sections with extension flaps, it was necessary to use theoretical calculation in analyzing the performance of propellers with these sections. The calculated and experimental values of α_{l_o} for the original sections are not in perfect agreement. Since experimental data were used for the original sections, the differences between the calculated values for the original and the extended airfoil section characteristics were applied to these experimental data. The corrected values were then used in calculating the performance of the propeller with extension flaps.

RESULTS AND DISCUSSION

Computations were made to determine the effect of the trailing-edge extension on the lift characteristics of an airfoil as a function of angle of attack. Curves showing the results of some of these computations are presented in figures 3 to 6. The calculated angle of zero lift α_{l_o}, the ideal angle of attack α_I, and $\alpha_I - \alpha_{l_o}$ (on which the design lift coefficient depends) are given for the propeller section at the

[redacted]

0.45 radius in figure 3. The calculated angles are measured from a straight line joining the extremities of the mean camber line of the extended airfoil section but are plotted against the angle between the extension flap and the straight line joining the extremities of the mean camber line of the original airfoil section, as was done in reference 1. The effects of a 10-percent extension, a 20-percent extension, and a 40-percent extension are compared.

In the use of this information for propeller calculations, it is more convenient to refer the calculated angles to the line joining the extremities of the mean camber line of the original airfoil section. The angular difference α_1 between the two reference lines is given by the following formula:

$$\tan^{-1}\alpha_1 = \frac{\left(\frac{\text{Extension length}}{\text{Chord}}\right) \sin (\text{Angle of extension})}{1 + \left(\frac{\text{Extension length}}{\text{Chord}}\right) \cos (\text{Angle of extension})}$$

The results for the 0.45 radius plotted in figure 3 are replotted in figure 4, but in figure 4 the calculated angles are measured from the chord line of the original airfoil section. The calculated and extrapolated experimental values of α_{l_o} and $\alpha_I - \alpha_{l_o}$ for the original section (without flap) are shown in figure 4. The points on the curves also show the calculated angles at which the extension flap must be set to the chord line of the original section to give the same value of α_{l_o} or $\alpha_I - \alpha_{l_o}$ for the extended section as for the original section. If the values of α_{l_o} for the sections with the extension flap are the same as for the original sections, the pitch distribution is unchanged. Since α_I for the original section (16 series) is zero, the crossing of the α_I curves with the zero ordinate gives the angle of extension for an unchanged α_I. Figure 5 shows similar curves for a 20-percent-chord extension flap and for a 40-percent-chord extension flap at the 0.95 radius. In figure 6 the curves at several radii are compared for the 20-percent-chord extension. From curves of this type, any desired change in the pitch distribution of a propeller may be made by properly setting the extension-flap angles.

[redacted]

Since the inboard sections of the original propeller stalled much earlier than the outboard sections for low V/nD operation, it was decided to change the angles of zero lift of the blade sections in order to shift more of the load toward the tip. This change in the angle of zero lift is obtained by setting the flap extension at the proper angle to the chord line. The angles of zero lift of the blade sections were changed by the amount shown by the solid line in figure 7. This curve may be shifted up or down, as is shown by the dashed lines in figure 7, with no change in the load distribution; the only changes resulting are in the design lift coefficients and a constant shift in the angles of zero lift of the sections. In making the propeller performance calculations, however, a shift in the angles of zero lift results in a change in the propeller pitch setting for constant C_P and V/nD. The only change in C_T and η will result from the small effect of the change in the drag of the airfoil sections.

Examination of the results (see figs. 4 to 6) shows that a 20-percent-chord extension to the Curtiss 836- or 837-1C2-13 blade should be set about 7.2° to the chord line at all blade sections to give the various angles of zero lift that would be obtained by adding $\Delta\alpha_{l_o}$ (solid line in fig. 7) to α_{l_o} of the original section. A 40-percent-chord extension should be set about 6.4° at all blade sections. The angles of zero lift for the sections at all radii given in figure 2 were increased by the amount shown by the solid line in figure 7 for making the calculations of the propeller performance with the extension flap.

Analyses of propeller performance for several propellers indicate that single-rotating propellers stall at section lift coefficients of about 1.0 for most of the blade and that the thin sections near the tip stall at section lift coefficients of 0.8 to 0.9. The calculations presented herein show that these lift coefficients were realized for a pitch setting of 24° at the 0.7 radius for operation at V/nD = 0.33 and that a 40-percent-chord extension (40-percent increase in solidity) is required to absorb the power. Experimental data on dual-rotating propellers, however, show that the dual-rotating propeller can be operated without stall at higher blade angles and at higher section lift

[redacted]

coefficients than single-rotating propellers. It is quite possible, therefore, that the 40-percent-chord flap extension to the tunnel propeller that would be required for a single-rotating propeller will not be necessary to prevent stall for the limiting condition of operation with dual-rotating propellers and that a lower solidity may be used. Nevertheless, in order to obtain conservative results, the calculations for the tunnel propeller have been made on the basis of a 40-percent-chord flap extension and the results for two operating conditions are given.

Figure 8 shows the differential thrust and torque curves plotted against x for operation at a V/nD of 0.33 with the front-propeller blade angle set 24° and the rear-propeller blade angle set 23° at the 0.7 radius. The element lift coefficients at several section radii are shown in this figure. Figure 9 shows similar curves for operation at V/nD = 0.26 with the front-propeller blade angle set 12° and the rear-propeller blade angle set 11° at the 0.7 radius.

CONCLUDING REMARKS

The solidity of a six-blade dual-rotating propeller having Curtiss 836- and 837-1C2-13 blades has been increased by adding extension flaps to the trailing edge. The method of analyzing the new blade-section characteristics in this case was applied to a particular propeller for operation at a very low advance-diameter ratio, but the method may be applied to any propeller section under any operating condition. The pitch distribution of the propeller with flaps may be held constant or, if desired, may be varied for different design operating conditions by properly setting the flap angle.

Langley Memorial Aeronautical Laboratory
National Advisory Committee for Aeronautics
Langley Field, Va.

[redacted]

REFERENCES

1. Theodorsen, Theodore, and Stickle, George W.: Effect of a Trailing-Edge Extension on the Characteristics of a Propeller Section. NACA ACR No. L4I21, 1944.

2. Stack, John: Tests of Airfoils Designed to Delay the Compressibility Burble. NACA TN No. 976, Dec. 1944. (Reprint of ACR, June 1939.)

[redacted]

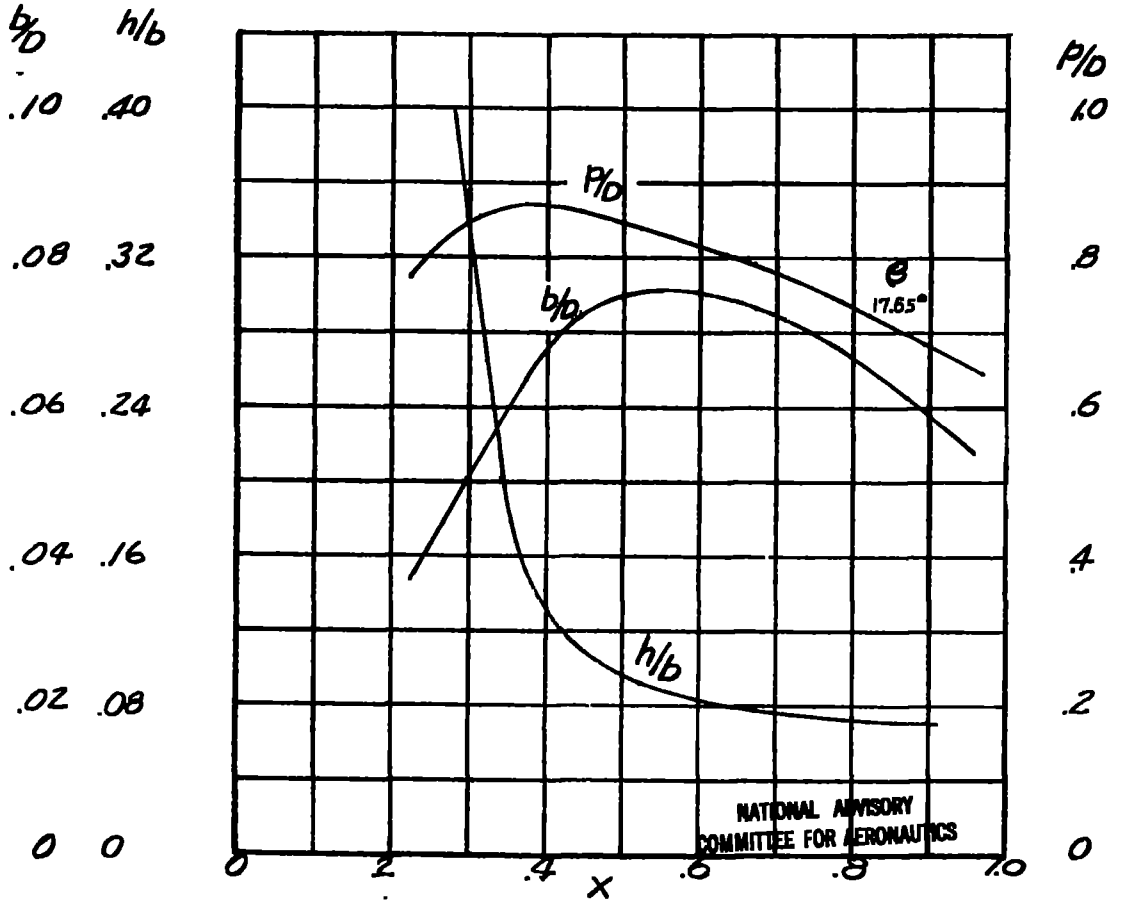

Figure 1.- Blade-form curves for dual-rotating propeller having Curtiss blades 836- and 837-1C2-13. Diameter, 13 feet 5 inches.

[redacted]

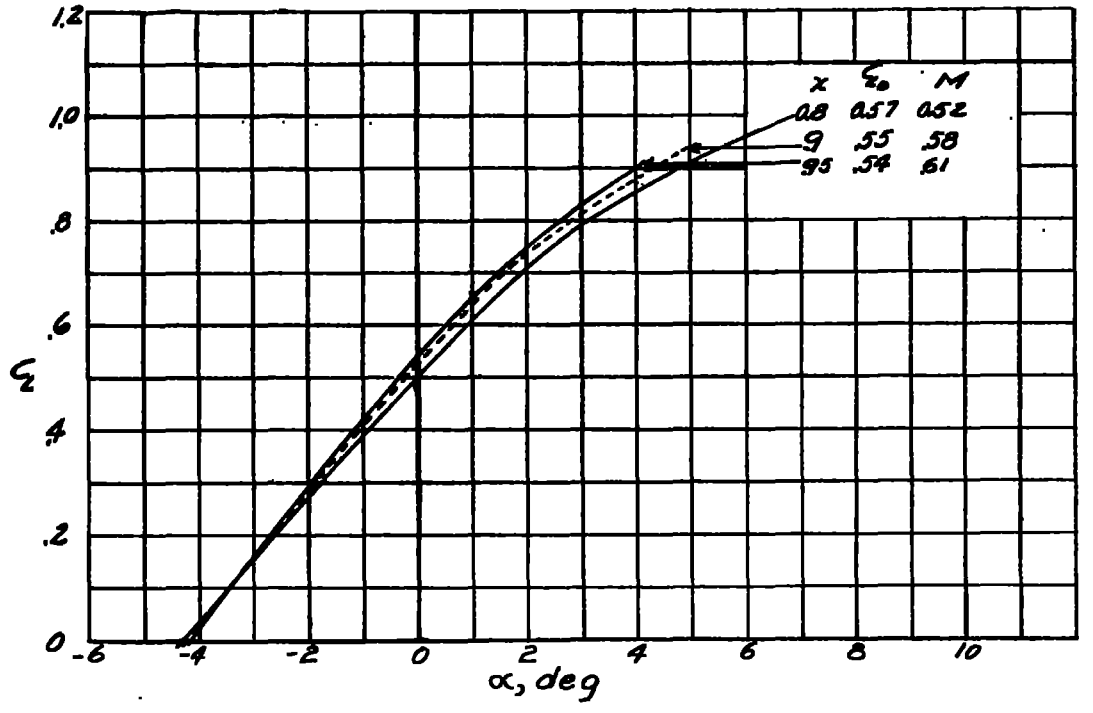

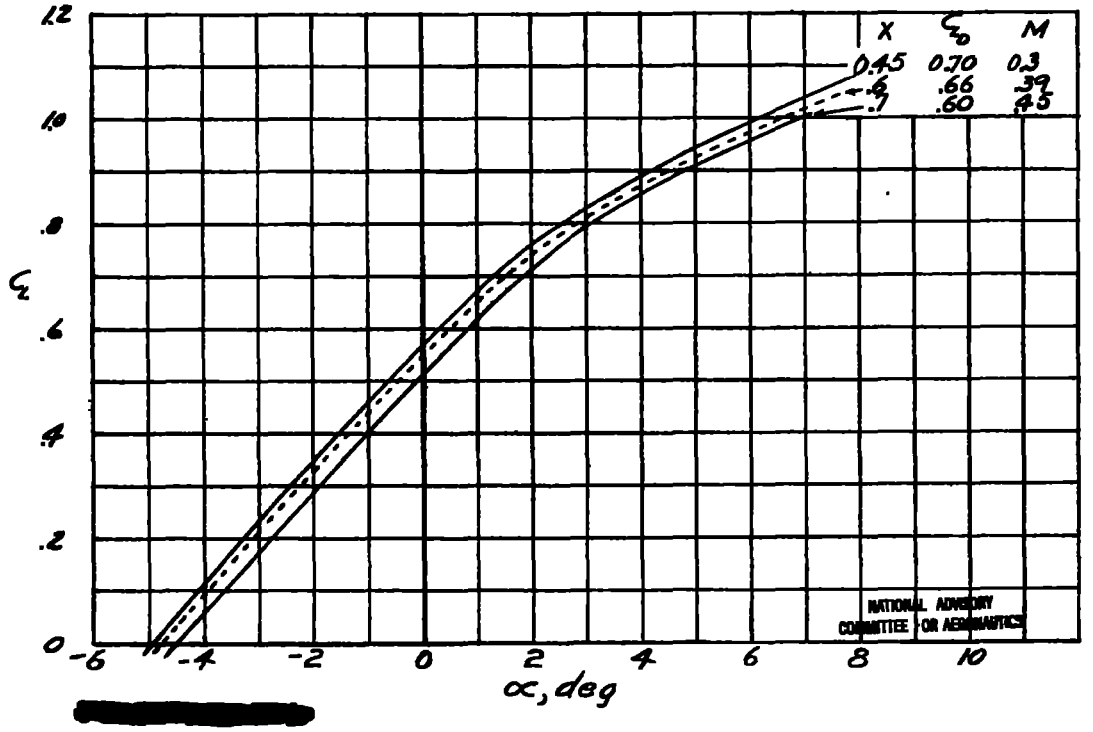

[redacted]

Figure 2.- Lift characteristics for 16-series sections for original Curtiss propeller blades 836- and 837-102-13. Diameter, 13 feet 5 inches. Data extrapolated from reference 2.

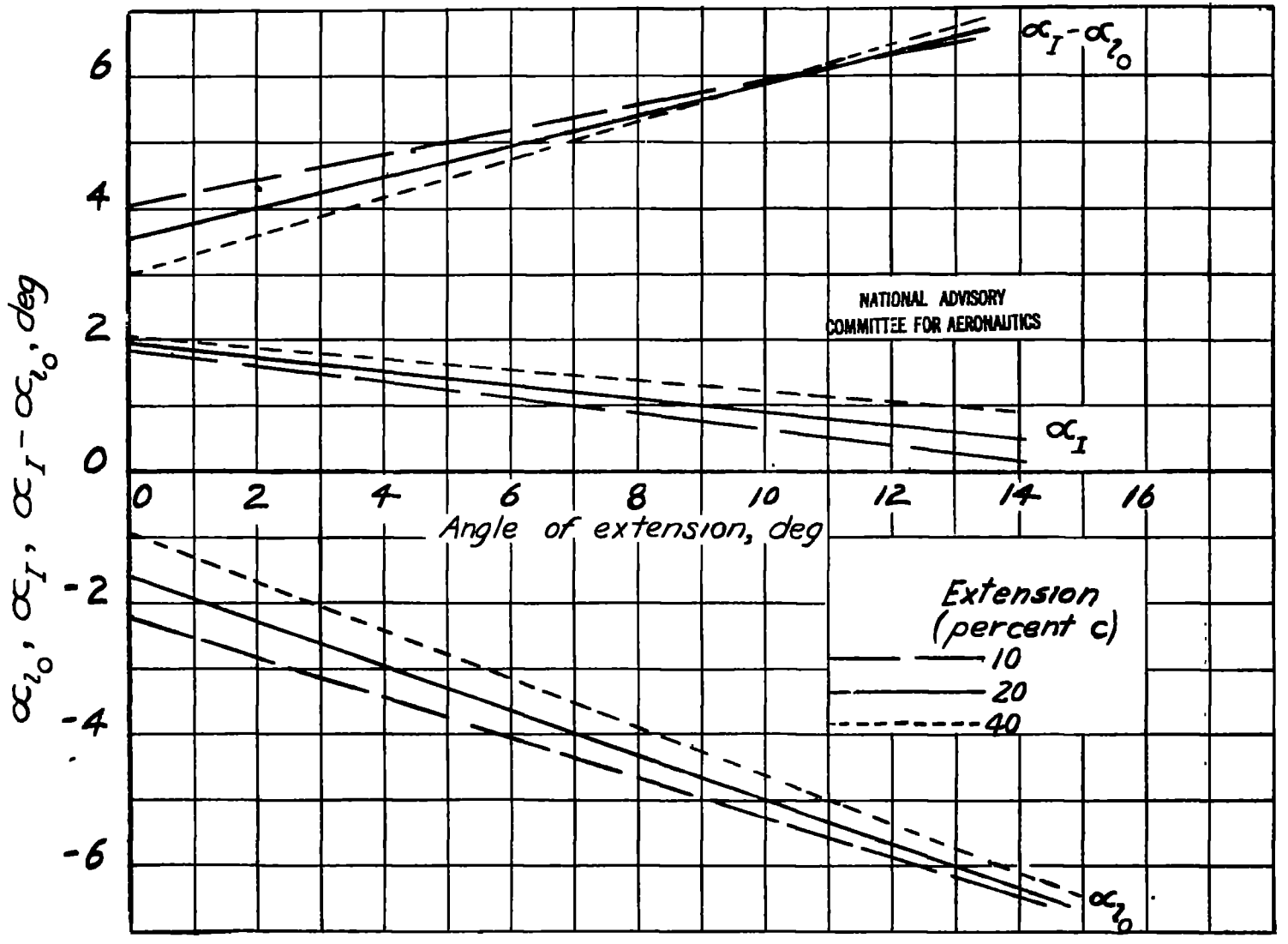

Figure 3.- Variation of α_{l_0}, α_I, and $\alpha_I - \alpha_{l_0}$ with angle of extension at $x = 0.45$.
(Angles measured from chord of extended airfoil.)

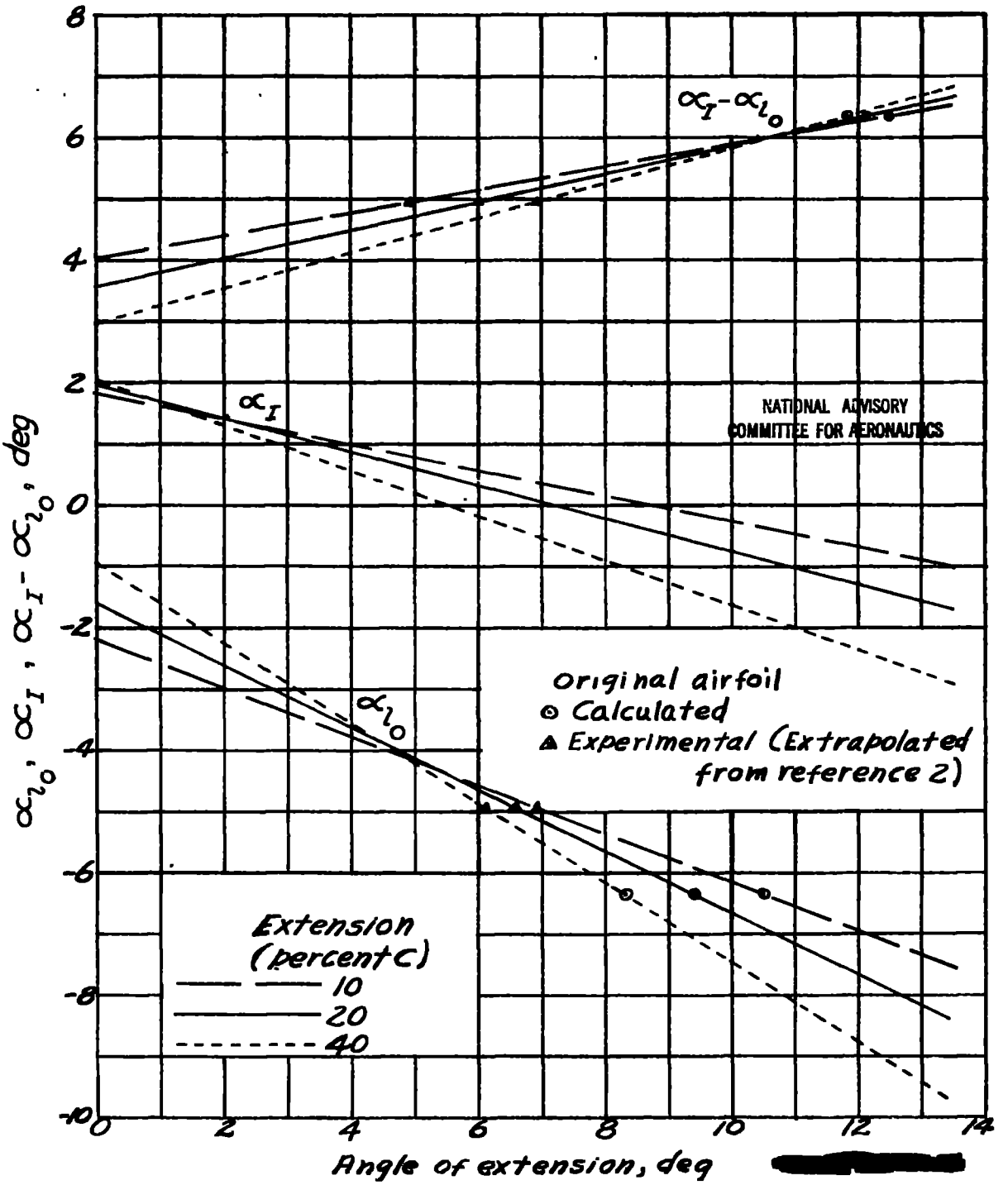

Figure 4.- Variation of α_{l_o}, α_I, and $\alpha_I - \alpha_{l_o}$ with angle of extension at x = 0.45. (Angles measured from chord of original airfoil.)

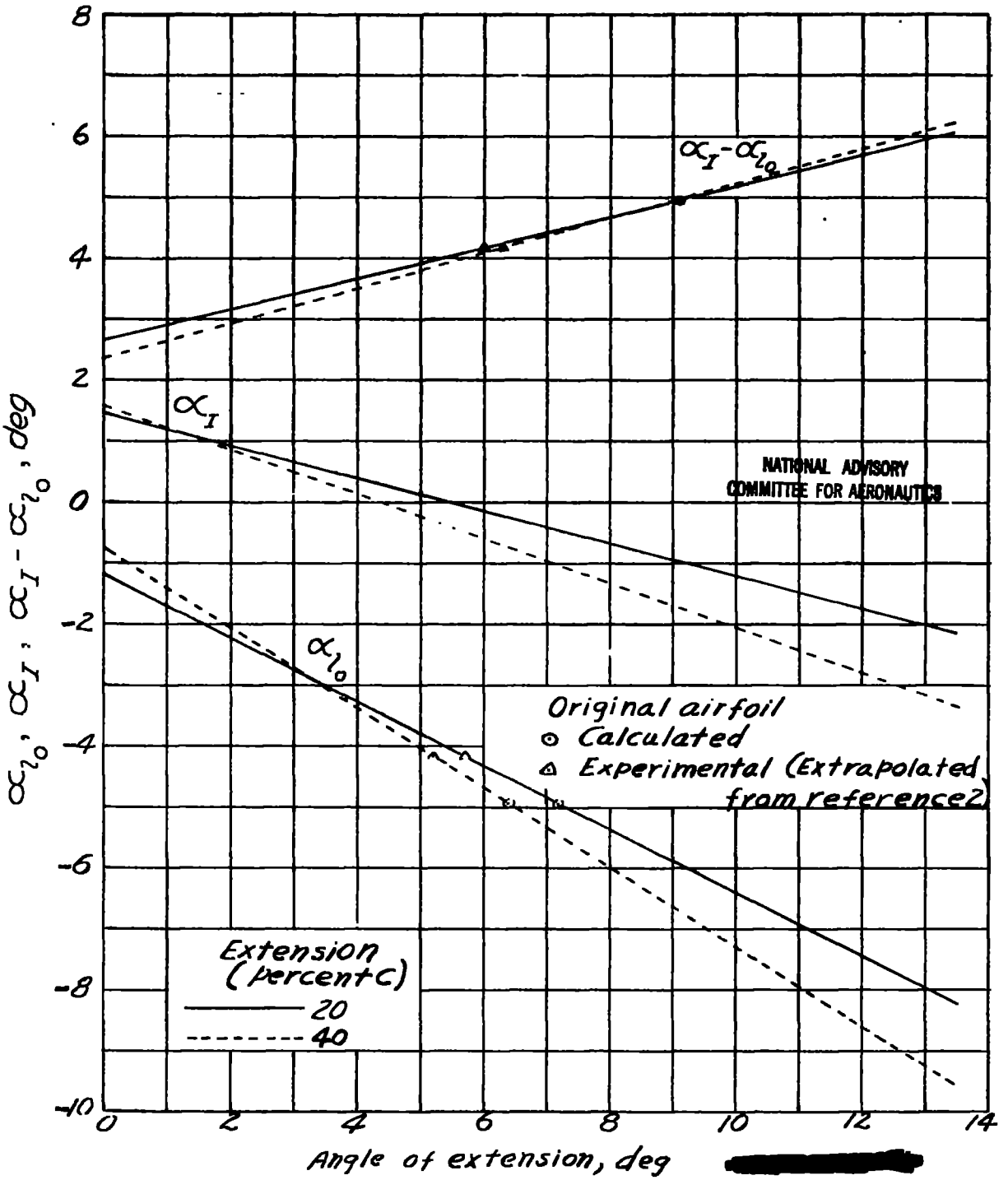

Figure 5.- Variation of α_{l_0}, α_I, and $\alpha_I - \alpha_{l_0}$ with angle of extension at x = 0.95. (Angles measured from chord of original airfoil.)

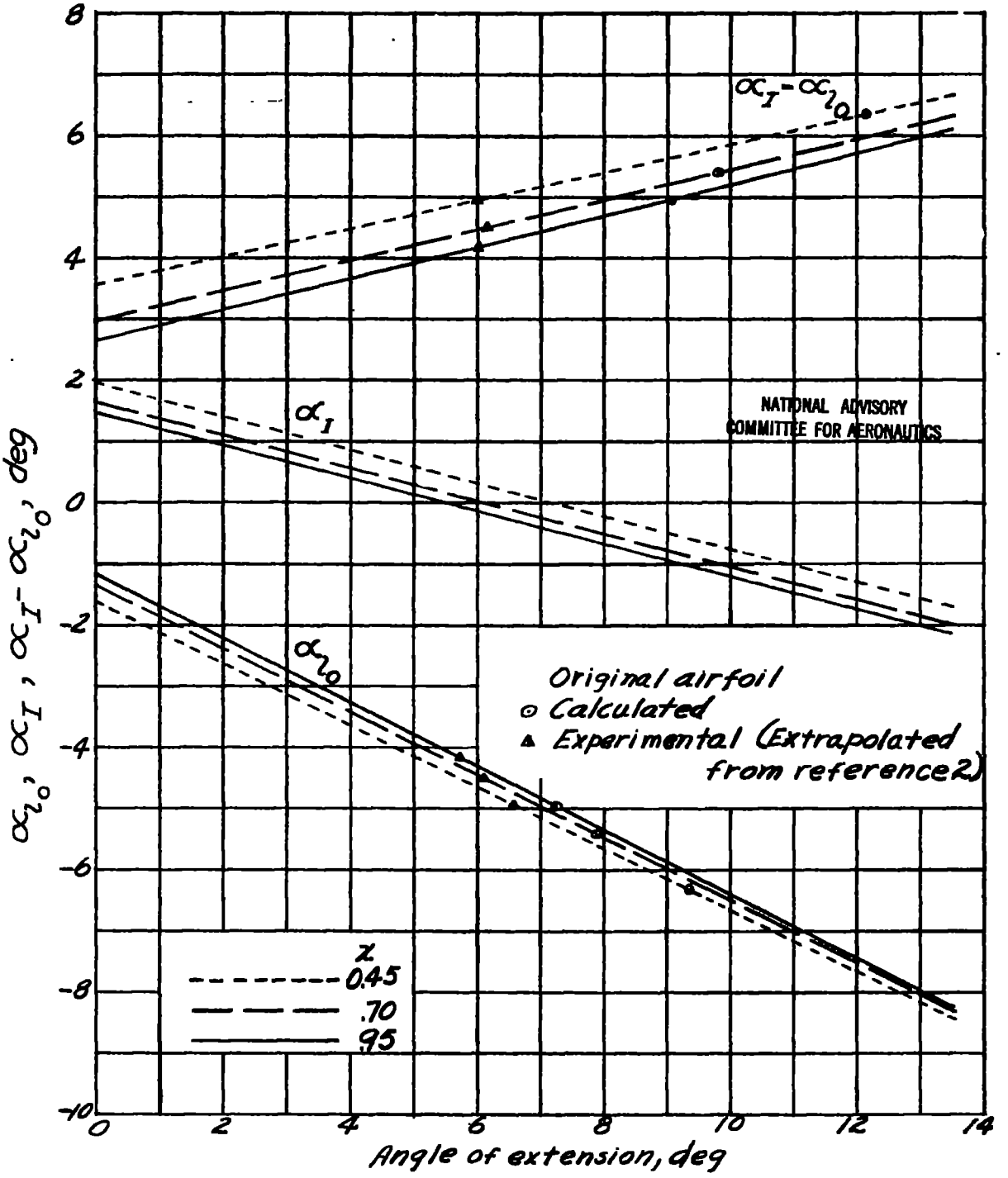

Figure 6.- Variation of α_{l_0}, α_I, and $\alpha_I - \alpha_{l_0}$ with angle of extension for 20-percent-chord extension flap. (Angles measured from chord of original airfoil.)

[redacted]

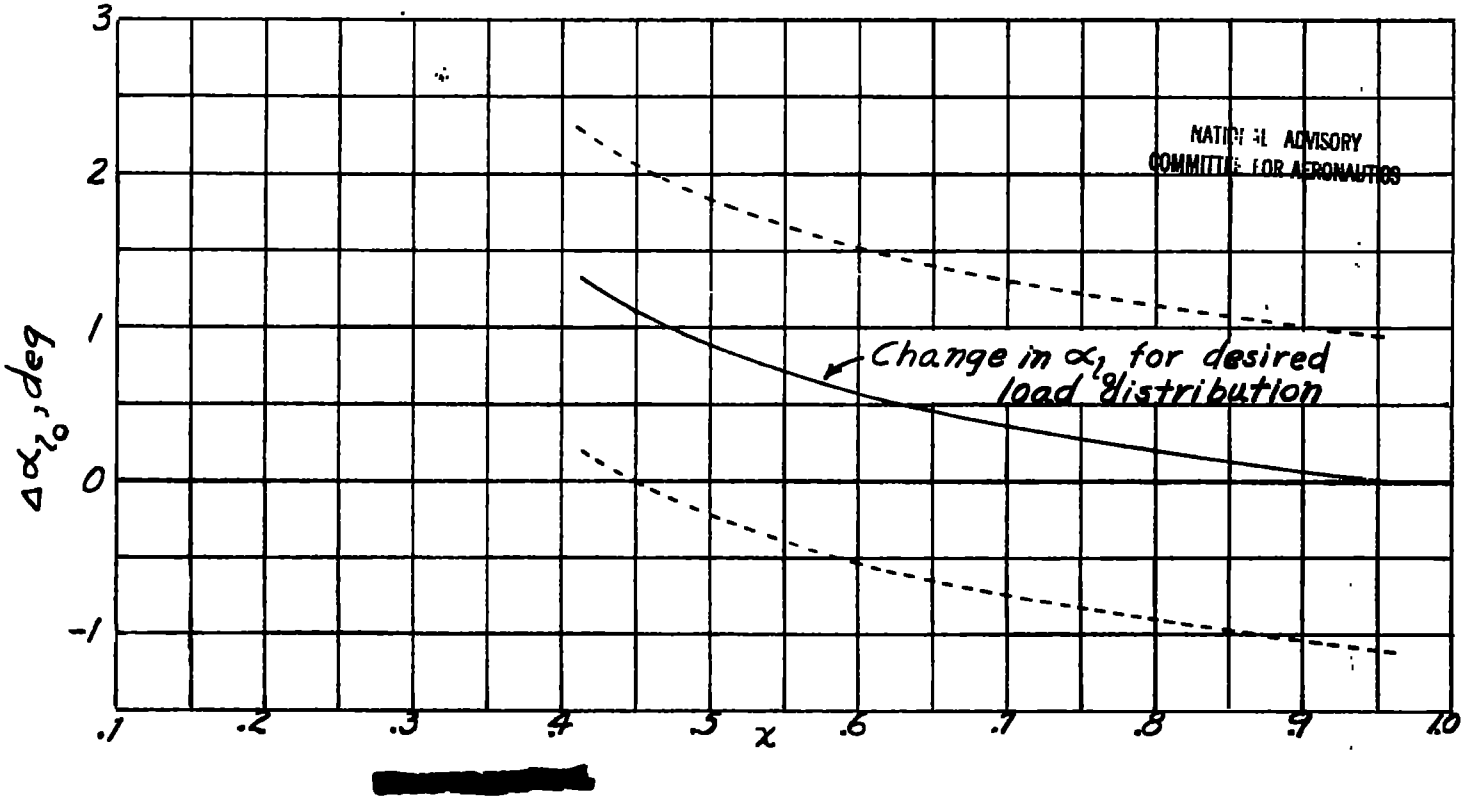

Figure 7.- Change in angle of zero lift due to chord extension for sections of dual-rotating propeller having Curtiss blades 836- and 837-102-13.

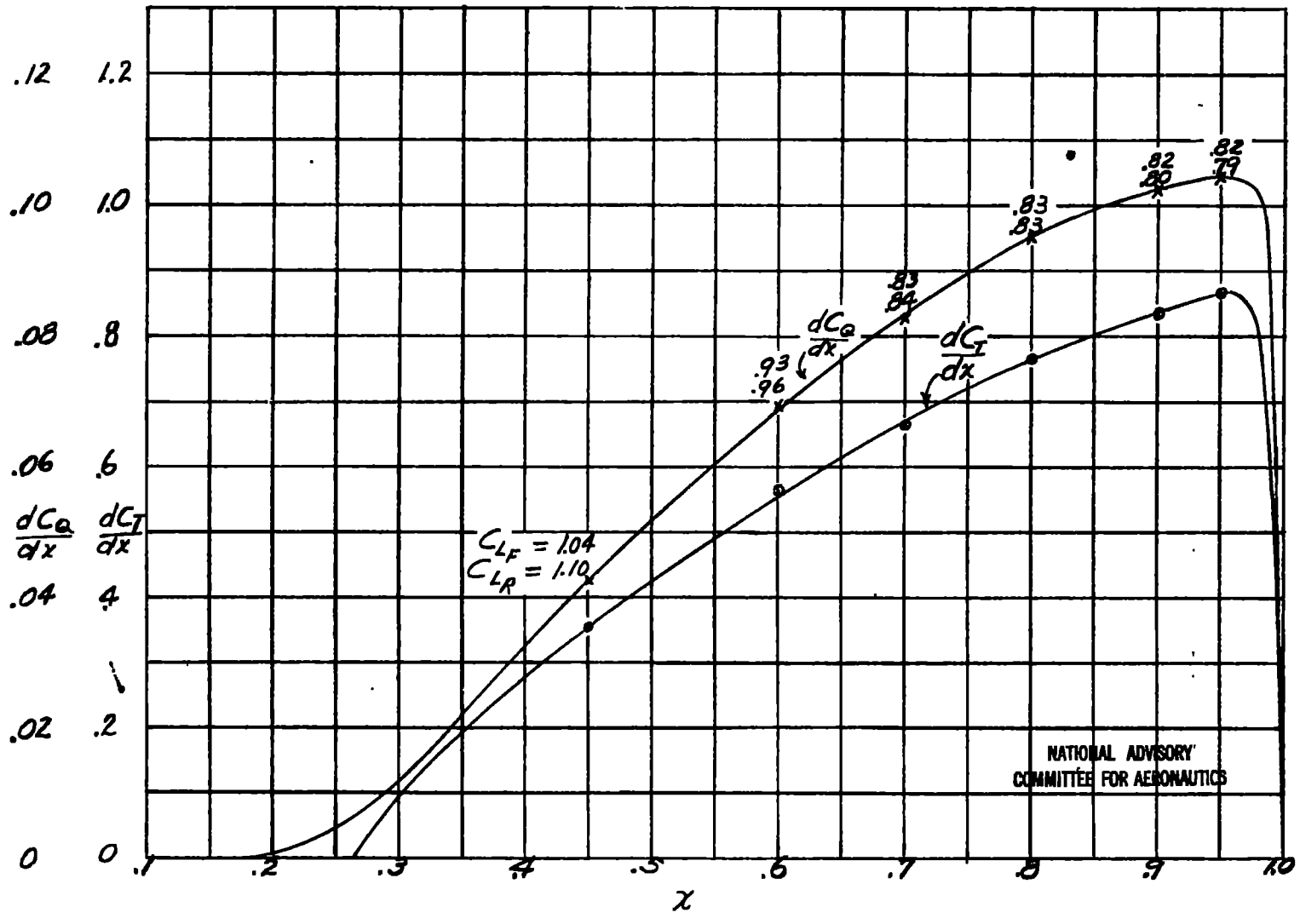

Figure 8.- Differential thrust and torque curves for six-blade dual-rotating propeller with Curtiss blades 836- and 837-102-13 with 40-percent-chord extension flap. V/nD = 0.33; $\theta_{0.7_F} = 24^\circ$; $\theta_{0.7_R} = 23^\circ$; $C_P = 0.310$; $C_T = 0.396$.

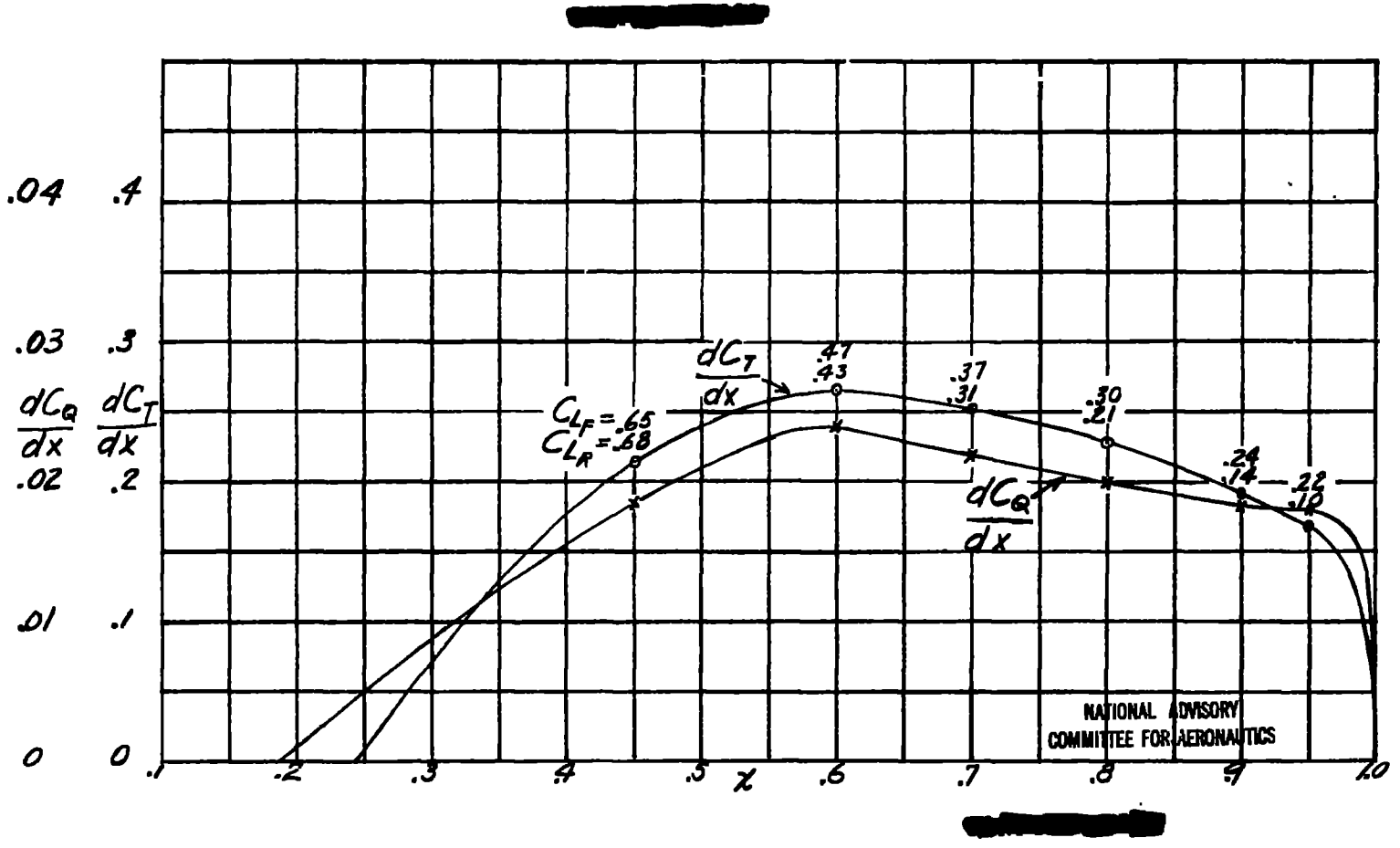

Figure 9.- Differential thrust and torque curves for six-blade dual-rotating propeller with Curtiss blades 836- and 837-102-13 with 40-percent-chord extension flap. V/nD = 0.26; $\theta_{0.7_F} = 12^\circ$; $\theta_{0.7_R} = 11^\circ$; $C_P = 0.0868$; $C_T = 0.1497$.